Periodic Sources of Gravitational Radiation

Sept. 2000

Contents

1 Introduction

Periodic gravitational waves are emitted in many processes involving isolated stars or binary systems. The emission of gravitational radiation determines an evolution of the emitting source (due to the *gravitational radiation reaction*) so that the amplitude and the frequency of the waves change with time. Thus, the so-called periodic sources are not truly periodic.

The emission of gravitational radiation dissipates the kinetic or internal energy of the star so that the final product of the evolution is an axisymmetric and/or non rotating object. Then, each source can be characterized by a decay time, the time during which gravitational waves are emitted (it is determined, for instance, by the spin down rate for rotating neutron stars). Here, we are interested in those periodic sources which radiate in the sensitivity band of forthcoming laser interferometers: they essentially involve compact objects, namely neutron stars. The number of neutron stars in the Galaxy has been estimated to be of the order of 10^9, with a comparable number of stellar mass black holes [8], [9]. The number of *observed* neutron star is much lower: about 800 are observed as radio pulsars [17], about 150 as X-ray binaries [1] and a few as isolated neutron stars (emitting X-rays) [2]. In the Galaxy, $\sim 2 \cdot 10^5$ active pulsars are expected to exist[69].

In this review we will briefly describe the different known processes in which periodic waves are produced, considering the characteristic timescales on which radiation is emitted and on which the frequency of the signal changes, and giving estimations of the expected amplitude of the signals.

Schematically, periodic sources in the interferometers band can be divided in

- Isolated rotating neutron stars;
- Accreting neutron stars.

2 The structure of neutron stars

Neutron stars are the outcome of the gravitational collapse of massive stars, with initial mass greater than $\sim 8 \div 10\ M_\odot$, or of accreting white dwarfs. Immediately after the collapse a differentially rotating proto-neutron stars forms, with a radius $\sim 100\ km$ and a temperature $T \sim 10^{12}\ K$. The proto-neutron

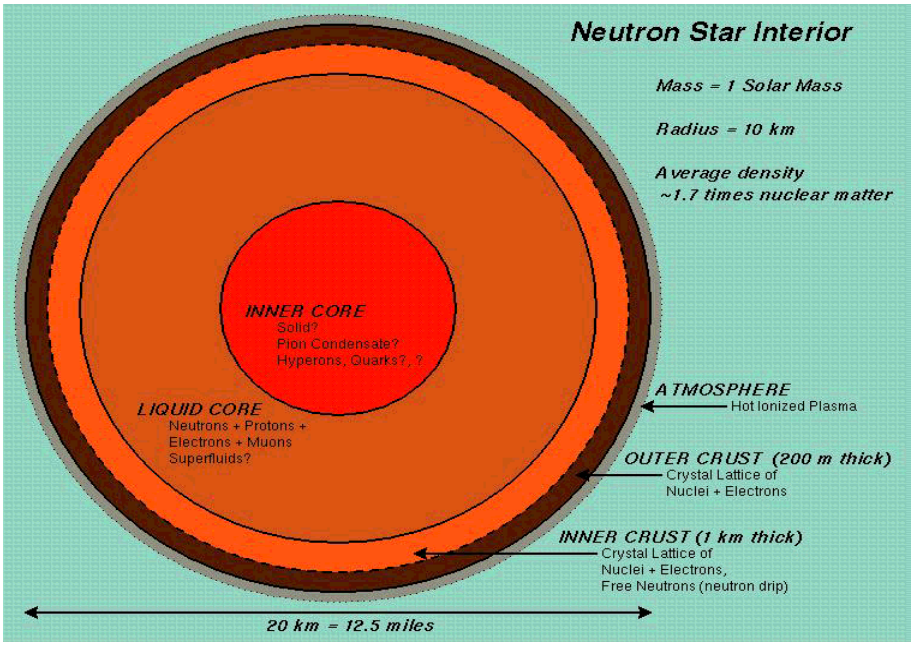

Figure 1: The structure of neutron stars. Picture taken at the *Marshall Space Flight Center* web site http://xanth.msfc.nasa.gov/xray/openhouse/ns/.

star rapidly cools and contracts (with a timescale of $\sim 20\ s$ at most), due to neutrino emission, forming a hot neutron star with temperature $T \sim 10^{11}\ K$ and radius $R \sim 10\ km$. With a typical mass $M \simeq 1.4\ M_{\odot}$, the mean density is $\overline{\rho} \simeq 10^{15}\ g/cm^3$. At the same time, viscosity reduces the differential rotation to a nearly uniform rotation [3]. The matter is a mixed plasma of atomic nuclei, neutrons, protons and electrons. After $\sim 1\ min$, when temperature reach $T \sim 10^{10}\ K$, the external layers begins to solidify: the resulting crust (*outer crust* in Fig.(1)) is composed of a body centered cubic lattice of nuclei, immersed in a uniform background of electrons [13]. Going deeper in the neutron star the neutron fraction in nuclei increases and above the so-called *neutron drip* density, $\rho_{ND} \sim 5 \cdot 10^{11}\ g/cm^3$, an increasing number of neutrons form a gas outside

the lattice of nuclei (*inner crust* in Fig.(1)). At still higher densities the solid phase is no longer present and for $\rho \gtrsim 10^{14}\ g/cm^3$ matter becomes a homogeneus mixture of neutrons, protons and electrons (*liquid core* in Fig.(1)), probably in a superfluid phase [4], [56]. According to some, still rather uncertain, models [5], [6], [7] neutron stars could have also a central solid core, at densities $\gtrsim 10^{15}\ g/cm^3$, as a consequence of specific features of nucleon-nucleon strong interactions.

3 Isolated neutron stars

Isolated rotating neutron stars emit gravitational radiation if their configuration is not axisymmetric with respect to the rotation axis. The asymmetry can be a consequence of deformations of the star shape or of a tilting of the symmetry axis with respect to the rotation axis.

In the following sections we will give general expressions, within the quadrupole formalism, for the waveforms and the power emitted by a source of gravitational radiation. Then, in Sec.(3.1,3.2), we will apply these relations to the two basic configurations of a rotating star:

- Rotation around a principal axis of inertia;
- Rotation around an axis different from a principal axis of inertia;

In Sec.(3.3) we will shortly describe some mechanisms which can produce an asymmetry in the shape of a neutron star. Finally, in Sec.(3.4) we will consider the growing of non-axisymmetric secular instabilities in rotating neutron stars, connected with gravitational radiation reaction and viscosity.

A general expression for the gravitational waveform emitted by a nonaxisymmetric rotating star can be derived in the framework of the quadrupole formalism. This applies when the size of the source, R, is much smaller than the reduced wavelenght, $\frac{\lambda}{2\pi}$, of the radiation it emits [10]:

$$\frac{2\pi R}{\lambda} \ll 1 \tag{1}$$

This is called *slow motion approximation*[1]. In the case of a fast rotating neutron

[1]Considering that the tangential velocity of the star is $v = \pi R\nu$, where ν is the frequency of the gravitational waves emitted, and that the wavelenght of radiation is $\lambda = \frac{2c}{\nu}$, the condition given by Eq.(1) is equivalent to

$$v << c \tag{2}$$

star with $R \sim 10\ km$ emitting gravitational radiation with frequency $\nu \sim 1000\ Hz$ we have $\frac{2\pi R}{\lambda} \sim 0.2$ so that the condition is marginally verified.

In this formalism, and using the *transverse-traceless gauge* (TT-gauge), the i, j component of the tensor describing the gravitational wave is

$$h_{ij}^{TT}\left(t - \frac{r}{c}\right) = \frac{2}{r}\frac{G}{c^4}\ddot{\mathcal{I}}_{ij}^{TT}\left(t - \frac{r}{c}\right) \tag{3}$$

where r is the distance from the source. Far from the source we can choose a reference frame whose z-axis is directed along the direction of propagation of the wave, in such a way that

$$h_{ij}^{TT} = h_+ e_{ij}^+ + h_\times e_{ij}^\times \tag{4}$$

where the polarization tensors $e_{ij}^+,\ e_{ij}^\times$ are defined by $e_{xx}^+ = -e_{yy}^+ = 1$, $e_{xy}^\times = e_{yx}^\times = 1$. Eq.(4) means that in the TT-gauge the gravitational wave has only two indipendent components corresponding to two polarization states.

The mean power emitted in gravitational radiation, averaged over the solid angle and over time, is given by

$$\frac{dE}{dt} = -\frac{G}{5c^5} < \frac{d^3\mathcal{I}_{\ ij}}{dt^3}\frac{d^3\mathcal{I}_{\ ij}}{dt^3} > \tag{5}$$

while the mean angular momentum carried off by gravitational waves is

$$\frac{dJ_i}{dt} = -\frac{2G}{5c^5}\epsilon_{ijk} < \frac{d^2\mathcal{I}_{\ jn}}{dt^2}\frac{d^3\mathcal{I}_{\ kn}}{dt^3} > \tag{6}$$

where $\epsilon_{ijk} = 1\ (-1)$ for an even (odd) permutation of the indexes $1, 2, 3$ and zero otherwise.

$\mathcal{I}^{TT}{}_{ij}$, which appear in Eq.(3), is the TT component of the mass quadrupole moment tensor of the source $\mathcal{I}_{\ ij}$:

$$\mathcal{I}^{TT}{}_{ij} = \left[P_k^i P_l^j - \frac{1}{2}P_{kl}P^{ij}\right]\mathcal{I}_{\ ij} \tag{7}$$

being P^{ij} the projection tensor transverse to the line of sight. The meaning of $\mathcal{I}_{\ ij}$, which is symmetric and trace-free, is clear when the source has weak internal gravity and stresses so that General Relativity can be replaced by Newtonian gravity. In such a case

$$\mathcal{I}_{\ ij} = I_{ij} \equiv \int \rho\left[x_i x_j - \frac{1}{3}\delta_{ij}r^2\right]dV \tag{8}$$

The weakness of the internal field can be expressed as a condition on the "relativistic factor" $\frac{GM}{Rc^2}$:

$$\frac{GM}{Rc^2} \ll 1 \tag{9}$$

For a neutron star with $M = 1.4\ M_\odot$ and $R = 10\ km$ we have $\frac{GM}{Rc^2} \simeq 0.2$.

When the source has strong internal gravity, the mass quadrupole moment cannot be expressed as an integral like that of Eq.(8) but in the slow-motion limit (i.e. $R \ll \lambda/2\pi$, or, equivalently, $v \ll c$) it can be obtained taking the coefficient of the quadrupolar part of the $\frac{1}{r^3}$ term in the expansion in powers of $\frac{1}{r}$ of the metric coefficient g_{00} when it is considered in an "asymptotically Cartesian and mass centered coordinate system" (ACMC) [11], [12]. In such a reference frame we can write, in the weak-field near zone, defined by $R \lesssim r \ll \lambda$, [11]

$$g_{00} = -1 + 2\frac{M}{r} + \frac{\alpha_1}{r^2} + \frac{1}{r^3}\left(3\mathcal{I}_{ij}\frac{x^i x^j}{r^2} + \beta_{1i}\frac{x^i}{r} + \alpha_2\right) + \mathcal{O}\left(\frac{1}{r^4}\right) \simeq -1 - 2\Phi \quad (10)$$

where $\alpha_1,\ \alpha_2,\ \beta_{1i}$ are coefficients and Φ is the Newtonian potential.

3.1 Rotation around a principal axis of inertia

Let us consider a rigid body rotating, say, around its 3^{rd} principal axis of inertia with angular velocity Ω . It is very easy to find, by the use of Eq.(8), the following expressions for the components of the tensor I_{ij} :

$$I_{11} = \frac{1}{2}cos(2\Omega t)(I_2 - I_1) - \frac{1}{6}(I_1 + I_2 - 2I_3)$$

$$I_{22} = \frac{1}{2}cos(2\Omega t)(I_1 - I_2) - \frac{1}{6}(I_1 + I_2 - 2I_3)$$

$$I_{33} = \frac{1}{3}(-2I_1 + I_2 + I_3)$$

$$I_{12} = I_{21} = \frac{1}{2}sin(2\Omega t)(I_2 - I_1) + \frac{1}{3}(I_1 + I_2 + I_3) \quad (11)$$

while all the other components are zero. The quantity I_1, I_2, I_3 are the principal moments of inertia of the body. If the rotating body can be approximated by a homogeneus ellipsoid of mass M with semiaxes a_1, a_2, a_3 then $I_1 = \frac{M}{5}(a_2^2 + a_3^2)$, and similarly for the other moments.

In the case of weak internal gravity, calculating the TT components of $\mathcal{I}_{ij}$, Eq.(7), and applying Eq.(3), we find

$$h_+ = \frac{h_0}{2} \cdot \cos 2\Omega t \left(1 + \cos^2\alpha\right) \quad (12)$$

$$h_\times = h_0 \cdot \sin 2\Omega t \cos\alpha \quad (13)$$

where we indicate with α the angle between the rotation axis and the line of sight and

$$h_0 = \frac{4G}{c^4 r}(I_1 - I_2)\Omega^2 \tag{14}$$

From Eqs.(12,13). we see that gravitational waves are emitted, if the body is not axisymmetric with respect to the rotation axis, i.e. if $I_1 \neq I_2$, at twice the rotation frequency. Defining the *ellipticity* ϵ as

$$\epsilon = \frac{I_1 - I_2}{I_3} \tag{15}$$

we can write

$$h_0 = 1.05 \cdot 10^{-27} \left(\frac{I_3}{10^{38}\ kg\ m^2}\right) \left(\frac{10\ kpc}{r}\right) \left(\frac{\nu}{100\ Hz}\right)^2 \left(\frac{\epsilon}{10^{-6}}\right) \tag{16}$$

where $\nu = \frac{\Omega}{\pi}$ is the gravitational wave frequency. From Eq.(5) we find for the power emitted

$$\frac{dE}{dt} = -\frac{32}{5}\frac{G}{c^5} I_3^2 \epsilon^2 \Omega^6 \tag{17}$$

From Eq.(6) we can easily calculate the star slow-down as it emits gravitational waves. Under the hypothesis that the star shape remains unchanged (it may change, for instance, as a consequence of star-quakes, see Sec.(3.3)) the only time-dependent component of the star angular momentum is J_3 :

$$\frac{dJ_3}{dt} = \frac{1}{\Omega}\frac{dE}{dt} = I_3 \cdot \dot{\Omega} = -\frac{32}{5}\frac{G}{c^5} I_3^2 \epsilon^2 \Omega^5 \tag{18}$$

hence

$$\dot{\nu} = -\frac{32\pi^4}{5}\frac{G}{c^5} I_3 \epsilon^2 \nu^5 = -1.7 \cdot 10^{-14} \left(\frac{I_3}{10^{38}\ kg\ m^2}\right) \left(\frac{\epsilon}{10^{-6}}\right)^2 \left(\frac{\nu}{100\ Hz}\right)^5 \quad s^{-2} \tag{19}$$

where ν is the frequency of the gravitational signal emitted, or, equivalently

$$\dot{P} = 2.74 \cdot 10^{-17} \left(\frac{I_3}{10^{38}\ kg\ m^2}\right) \left(\frac{\epsilon}{10^{-6}}\right)^2 \left(\frac{P}{.01s}\right)^{-3} \quad s/s \tag{20}$$

The right-hand side of Eq.(18) is the *gravitational torque* acting on the pulsar, responsible for the star spin-down. The characteristic spin-down age is defined as[2]

$$t_{sd} = \frac{P}{\dot{P}} = -\frac{\nu}{\dot{\nu}} = \frac{5c^5 P^4}{128\pi^4 G I_3 \epsilon^2} \simeq 1.2 \cdot 10^7 \left(\frac{I_3}{10^{38} kg \cdot m^2}\right)^{-1} \left(\frac{\epsilon}{10^{-6}}\right)^{-2} \left(\frac{P_0}{.01s}\right)^4 \ yr \tag{21}$$

[2]It would be four times the life-time of the pulsar, if the initial period P_0 was much shorter than P and the star would slow-down only due to a constant gravitational torque.

In the case of sources with strong internal gravity, for which Eq.(8) cannot be applied, it is still possible to express the amplitudes of the two polarization states of the wave and the power emitted through Eqs.(12,13,16,17) defining the ellipticity as

$$\epsilon = \frac{\mathcal{I}_{\hat{1}\hat{1}} - \mathcal{I}_{\hat{2}\hat{2}}}{I_3} \tag{22}$$

where the components of the mass quadrupole moment tensor are calculated along the principal axis of inertia in the plane perpendicular to the rotation axis. In the weak field limit $\mathcal{I}_{\hat{1}\hat{1}} - \mathcal{I}_{\hat{2}\hat{2}} \to I_1 - I_2$.

3.2 Rotation around an axis different from a principal axis of inertia

As a consequence of star-quakes, strong internal magnetic fields or interactions with other stars, see Sec.(3.3) for more details, the rotation axis of a neutron star can be different from one of its principal axis of inertia. Two different cases have been analyzed in literature:

1. Precession of a rigid neutron star;

2. Rotation of a distorted fluid neutron star.

3.2.1 Precession of a rigid neutron star

Let us consider a rotating rigid neutron star with $I_1 = I_2 \neq I_3$. Let us indicate with $\vec{e_1}, \vec{e_2}, \vec{e_3}$ the principal axes of inertia of the star and with $\vec{e_x}, \vec{e_y}, \vec{e_z}$ the axes of an inertial reference frame. We assume that the angular momentum $\vec{J}$ is directed along $\vec{e_z}$. If the angular velocity vector $\vec{\omega}$ is not directed along $\vec{J}$, then a precession of $\vec{\omega}$, and $\vec{e_3}$, around $\vec{e_z}$, takes place with angular velocity $\Omega = \frac{J}{I_1}$.

The two polarization states of the gravitational wave emitted are [21]

$$h_+ = h_0 \sin\theta \left[\cos\theta \sin\alpha \cos\alpha \cos\Omega t + \sin\theta \left(1 + \cos^2\alpha\right) \cos 2\Omega t\right] \tag{23}$$

$$h_\times = h_0 \sin\theta \left[\cos\theta \sin\alpha \sin\Omega t + 2 \sin\theta \cos\alpha \sin 2\Omega t\right] \tag{24}$$

where θ , called *wobble angle*, is the angle between $\vec{e_z}$ and $\vec{e_3}$ while α is the angle between the rotation axis and the line of sight defined in such a way

that $\alpha = 0$ means that $\vec{J}$ point toward the observer and $\alpha = \frac{\pi}{2}$ means that $\vec{J}$ is perpendicular to the observer. The amplitude of the wave is

$$h_0 = \frac{2G}{c^4}\frac{\epsilon I_1}{r}\Omega^2 \tag{25}$$

having defined the *ellipticity* as

$$\epsilon = \frac{(I_3 - I_1)}{I_1} \tag{26}$$

Note that gravitational radiation is emitted at two frequencies, Ω and 2Ω : the relative weight of the corresponding amplitudes depends on the angles α and θ. Eq.(25) can be rewritten, in terms of the frequency $\nu = \frac{\Omega}{2\pi}$, like Eq.(16):

$$h_0 = 1.05 \cdot 10^{-27} \left(\frac{I_1}{10^{38}\ kg\ m^2}\right) \left(\frac{10\ kpc}{r}\right) \left(\frac{\nu}{100\ Hz}\right)^2 \left(\frac{\epsilon}{10^{-6}}\right) \tag{27}$$

The angular velocity $\vec{\omega}$ is the sum of the precession velocity $\vec{\Omega}$, around $\vec{J}$, and of the intrinsic spin frequency of the star (also called *body frame precession frequency*), $\vec{\Omega}_s$, around its $\vec{e}_3$ axis:

$$\vec{\omega} = \Omega\vec{e}_z + \Omega_s\vec{e}_3 \tag{28}$$

The relation between Ω and ω is

$$\Omega\cos\theta = \frac{I_3}{I_1}\omega \tag{29}$$

while

$$\Omega_s = -\epsilon \cdot \omega_3 \tag{30}$$

where $\omega_3 = \vec{\omega} \cdot \vec{e}_3$. Then, tipically $\Omega_s \ll \omega$. The power emitted in gravitational waves is

$$\frac{dE}{dt} = -\frac{2G}{5c^5}(\epsilon I_1)^2 \sin^2\theta \left(16\sin^2\theta + \cos^2\theta\right)\Omega^6 \tag{31}$$

which, in the limit of small θ , can be written as

$$\frac{dE}{dt} \simeq -\frac{2}{5}\frac{G}{c^5}(\epsilon I_1)^2\theta^2\Omega^6 \tag{32}$$

It also rather easy to find the variation law for the wobblw angle θ:

$$\dot{\theta} = -\frac{2G}{5c^5}\epsilon^2 I_1 \sin 2\theta \left(16\sin^2\theta + \cos^2\theta\right)\Omega^4 \tag{33}$$

and the corresponding time-scale for the alignement between $\vec{e}_3$ and $\vec{e}_z$:

$$\tau_\theta = -\frac{\sin\theta}{\dot{\sin\theta}} = \frac{5c^5}{2G}\frac{1}{\epsilon^2 I_1 \cos^2\theta\left(16\sin^2\theta+\cos^2\theta\right)\Omega^4} \tag{34}$$

These relations can be extended to the case of a realistic neutron star, made of an elastic solid crust sorrounding a liquid interior, with the replacement

$$\epsilon^2 I_1 = \frac{(I_3-I_1)^2}{I_1} \rightarrow \frac{(I_3-I_1)_d^2}{I_{crust}} \tag{35}$$

where the suffix d denotes the deformation not due to rotation (i.e. that remains different from zero also in the non rotating limit) [22]. In this case, the fluid angular velocity vector does not significantly partecipate in the free precession. In the limit $\theta \ll 1$ the corresponding timescale for the alignement between $\vec{e}_3$ and $\vec{e}_z$ is

$$\tau_\theta = 1.8\cdot 10^9 \left(\frac{\epsilon_d}{10^{-6}}\right)^{-1}\left(\frac{\nu}{100\ Hz}\right)^{-4}\ yr \tag{36}$$

with $\epsilon_d = \frac{(I_3-I_1)_d}{I_{crust}}$. Note that depending on the sign of ΔI_d (>0: oblate configuration, <0: prolate configuration), the wobble angle increase or decrease in time. It is difficult to give firm theoretical upper limits on the *wobble angle* θ which a neutron star can sustain [13]. Anyway, we can expect $\theta \lesssim 10^{-2} \div 10^{-3}$ [60].

3.2.2 Rotation of a distorted fluid neutron star

Let us consider now a fluid rotating neutron star distorted along some direction, different from the direction of the rotation axis of the star. The misalignment between the two axes can be due to a torque produced by the neutron star magnetic field or by the tidal forces by a close companion star. A misalignment of the magnetic axis with respect to the rotation axis is widely assumed in order to explain the pulsar emission mechanism. For a liquid neutron star rotation contributes to affect the star shape: the distortion axis, in general, will not coincide with a pricipal axis of inertia[3]. Moreover, in this case the angular velocity vector is directed along the total angular momentum, then no precession occurs.

If the internal gravity is weak we have[4] [12]

$$h_+ = \frac{h_0}{2}\sin\theta\left[\frac{1}{2}\cos\theta\sin 2\alpha\cos\Omega t + \sin\theta\left(1+\cos^2\alpha\right)\cos 2\Omega t\right] \tag{37}$$

[3]Unless the magnetic distortion is very large with respect to that induced by rotation, as it could happen in *magnetars* [18].

[4]Eqs.(37, 38) are written using the same conventions of ref.([21]), see the discussion in sec.(2.4) of ref.([12]).

$$h_\times = h_0 \sin\theta \left[\frac{1}{2}\cos\theta \sin\alpha \sin\Omega t - \sin\theta\cos\alpha\sin 2\Omega t\right] \tag{38}$$

where θ is the angle between the rotation axis and the distortion axis ($\theta = 0, \pi$ if the two axis are alligned, $\theta = \frac{\pi}{2}$ if they are perpendicular), α is the angle between the rotation axis of the star and the line of sight and Ω is the angular velocity of the distortion axis with respect to the rotation axis. Then, we see that, again, gravitational waves are emitted at two frequencies: $\frac{\Omega}{2\pi}$ and $\frac{\Omega}{\pi}$. For small values of θ the emission at frequency $\frac{\Omega}{2\pi}$ is dominant. The amplitude of the waves is

$$h_0 = \frac{2G}{c^4}\frac{\epsilon I_3}{r}\Omega^2 \tag{39}$$

where the *ellipticity* is now defined as

$$\epsilon = \frac{(I_3 - I_1)}{I_3} \tag{40}$$

The amplitude given by Eq.(39) can be written, also in this case, in the same form as Eq.(16):

$$h_0 = 1.05 \cdot 10^{-27}\left(\frac{I_3}{10^{38}\ kg\ m^2}\right)\left(\frac{10\ kpc}{r}\right)\left(\frac{\nu}{100\ Hz}\right)^2\left(\frac{\epsilon}{10^{-6}}\right) \tag{41}$$

with $\nu = \frac{\Omega}{2\pi}$.

The power emitted in gravitational waves, from Eq.(5), is

$$\frac{dE}{dt} = -2\frac{G}{c^5}(\epsilon I_3)^2 \sin^2\theta\left(\frac{1}{5} + 3\sin^2\theta\right)\Omega^6 \tag{42}$$

In the limit of small θ we find

$$\frac{dE}{dt} \simeq -\frac{2}{5}\frac{G}{c^5}(\epsilon I_3)^2\theta^2\Omega^6 \tag{43}$$

This relation appears to be identical to Eq.(32), but the meaning of the angle θ is different: here θ is the angle between the rotation and the distortion axes, while in Eq.(32) it is the angle between the direction of the angular momentum and the principal axis of inertia $\vec{e_3}$. If the star is fluid these angles are different, because the distortion axis does not coincide, except that in the non rotating case and for very strong magnetic fields, with a principal axis of inertia. The characteristic spind-down age is

$$t_{sd} = \frac{P}{\dot{P}} = -\frac{\nu}{\dot{\nu}} = \frac{5c^5P^4}{8\pi^4 G I_3 \epsilon^2}\frac{1}{\sin^2\theta\left(\frac{1}{5} + 3\sin^2\theta\right)} \tag{44}$$

The formulae related to the amplitude of gravitational waves and to the power emitted, Eqs.(41,42), hold also in the case of strong gravity (if the slow-motion approximation is still valid) replacing ϵI_3 with $-\frac{3}{2}\mathcal{I}^{dist}{}_{\hat{3}\hat{3}}$. $\mathcal{I}^{dist}{}_{\hat{3}\hat{3}}$ is the zz component of the mass quadrupole moment tensor, due to processes which distort the star (different from rotation), such as an internal magnetic field, and calculated in the reference frame whose z-axis is directed along the deformation axis of the star [12].

In the next section we will describe some possible mechanisms which could induce a deformation in the star shape or a tilting of the symmetry axis with respect to the rotation axis, and we will give estimations of the maximum expected ellipticity ϵ .

3.3 Deformation of the neutron star shape

According to Eqs.(17,31,42) a rotating neutron star emits gravitational radiation if it is nonaxisymmetric or if its symmetry axis is tilted with respect to the rotation axis.

This can be the consequence of irregularities in the star solid crust, of anisotropic stresses from nuclear interactions, of strong magnetic fields with symmetry axis different from the rotation axis or of interactions with another star.

The existence of a solid crust in neutron stars is well established on theoretical grounds [13] and there is also some observational evidence, connected with the observed glitches in pulsars, which could be the consequence of star-quakes taking place in the solid surface of the star, see Sec.(3.3.1) for more details. These would be cracks in the crust, due to sufficiently large stresses, and could determine permanent deformations.

Alternatively, irregularities or the tilting of the symmetry axis could be produced during the initial phase of the cooling of the neutron star, when the crust solidifies. Moreover, an ellipticity ϵ different from zero can also appear if neutron stars have a solid core, but this possibility is still uncertain. It is not easy to estimate the ellipticity produced in all these processes.

As we have said before, Sec.(3.2.2), a different possibility is that a non zero ellipticity is the result of the stresses induced by large internal magnetic fields. For a neutron star modeled as an incompressible fluid, the ellipticity is expected

to be [12]

$$\epsilon \propto \beta \left(\frac{R}{I}\right)^2 \mathcal{M}^2 \tag{45}$$

where β is a dimensionless coefficient which expresses the capability of the magnetic field in distorting the star structure and $\mathcal{M}$ is the magnetic dipole moment of the neutron star.

The value of the coefficient β is critical in determining the ellipticity. If the hypothesis of normal-matter (not superconducting) neutron star is done, the resulting ellipticity is very low, $\epsilon \sim 10^{-9} \div 10^{-13}$, even if realistic equations of state are used and "standard" values of the magnetic field strength are considered [12]. Better results are obtained assuming, for instance, that the interior of the neutron star is a type I superconductor ($\epsilon \lesssim 10^{-7}$) or considering also a stochastic distribution of the magnetic field inside the star ($\epsilon \lesssim 10^{-6}$) [12]. Much larger values of ϵ can be obtained for *magnetars*, which have magnetic fields in the range $10^{14} \div 10^{15}$ G and for which magnetic energy is dominant with respect to rotational energy.

The emission of gravitational radiation, which in general will sum to other mechanisms of dissipation, contributes to the loss of the rotational energy of the star. All this energy losses determine a decrease in the rotational period P with rate $\dot{P}$. Correspondingly, there is a slowdown of the angular velocity Ω of the star. A general expression for the variation of the angular velocity is

$$\dot{\Omega} \propto -\Omega^n \tag{46}$$

or, in terms of the period P

$$\dot{P} \propto P^{n-2} \tag{47}$$

where n is the *braking index*. From the measure of Ω, $\dot{\Omega}$, $\ddot{\Omega}$ we can deduce the value of n according to the relation, easily derived from Eq.(46),

$$n \equiv \frac{\Omega \ddot{\Omega}}{\left(\dot{\Omega}\right)^2} \tag{48}$$

The value of n depends on the mechanisms responsible for the period variations: for instance [26], $n = 3$ for magnetic dipole radiation, $n = 5$ for gravitational radiation, $n > 5$ for multipole electromagnetic radiation, $n > 3$ for magnetic field decay, $1 \leq n \leq 3$ for radial deformations of the magnetic field lines, $n < 3$ for pulsar wind and for relaxation of the neutron star equilibrium form.

Only four pulsars have measured values of n not dominated by timing noise [26],[27]: $n \simeq 2.51$ for the *Crab*, $n \simeq 2.28$ for $PSR\ 0540-69$, $n \simeq 2.837$ for $PSR\ 1509-58$ and $n \simeq 1.4$ for the *Vela*. For these pulsars the main contribution to the spin down is due to the electromagnetic radiation and magnetospheric acceleration of charged particles.

In general, we have $\dot{P}_{GW} \leq \dot{P}$. This implies, from Eq.(17), that

$$\epsilon_{eff} \leq \epsilon_{max} = 1.9 \cdot 10^{-9} \left(\frac{P}{1\ ms}\right)^{3/2} \left(\frac{\dot{P}}{10^{-19} s/\dot{s}}\right)^{1/2} \tag{49}$$

where a typical value $I = 10^{38}\ kg \cdot m^2$ has been used for the momentum of inertia of the star and $\epsilon_{eff} \equiv \epsilon$ if the neutron star rotates about a principal axis of inertia, while $\epsilon_{eff} \equiv \epsilon \cdot \theta$ if the principal axis of inertia (or the distortion axis) forms an angle θ with the rotation axis and $\theta \ll 1$.[5] The equality in Eq.(49) would hold if $\dot{P}_{GW} = \dot{P}$, that is, if the loss of rotational energy was due only gravitational radiation emission. For the Vela pulsar we have $\epsilon_{max} = 1.8 \cdot 10^{-3}$ while for the Crab pulsar $\epsilon_{max} = 7.5 \cdot 10^{-4}$. In general, for millisecond pulsars the upper limit is much lower and of the order of $10^{-8} \div 10^{-9}$, see Tab.(1). Indeed, the observed pulsars can be roughly divided into two groups [16]. Young isolated pulsars (period in the range $\sim 30\ ms \div 5\ s$) are characterized by low rotational frequencies and low spindown age $\tau = \frac{P}{\dot{P}} \sim 10^7\ yr$, so that, from Eq.(49), the inferred value of ϵ_{max} is high. On the other hand, older millisecond pulsars (periods in the range $1.5\ ms \div 30\ ms$) have higher frequencies and higher spindown age ($\tau \sim 10^9\ yr$), so that the corrisponding ϵ_{max} is lower, see Figs.(2,3). Most of these millisecond pulsars are in binary systems and it is generally believed that they spun up as a consequence of accretion of matter from the companion star, see Sec.(4.1).

The physical absolute upper limit to the ellipticity is uncertain but probably in the range $\epsilon_{max} \sim 10^{-4} \div 10^{-6}$, due to the maximum strain that the neutron star crust can sustain [55].

Young pulsars (characterized by slower rotation) are likely to deviate more

[5]For a deformed, not precessing, rotating neutron star, the general expression for the maximum ellipticity is

$$\epsilon_{max} = \frac{\dot{P} \sin^2\theta + \sqrt{(\dot{P})^2 \sin^4\theta + (2\pi)^4 \frac{128G}{5c^5} I_3 \sin^2\theta \frac{\dot{P}}{P^3}}}{(2\pi)^4 \frac{64G}{5c^5} I_3 \sin^2\theta P^{-3}} \tag{50}$$

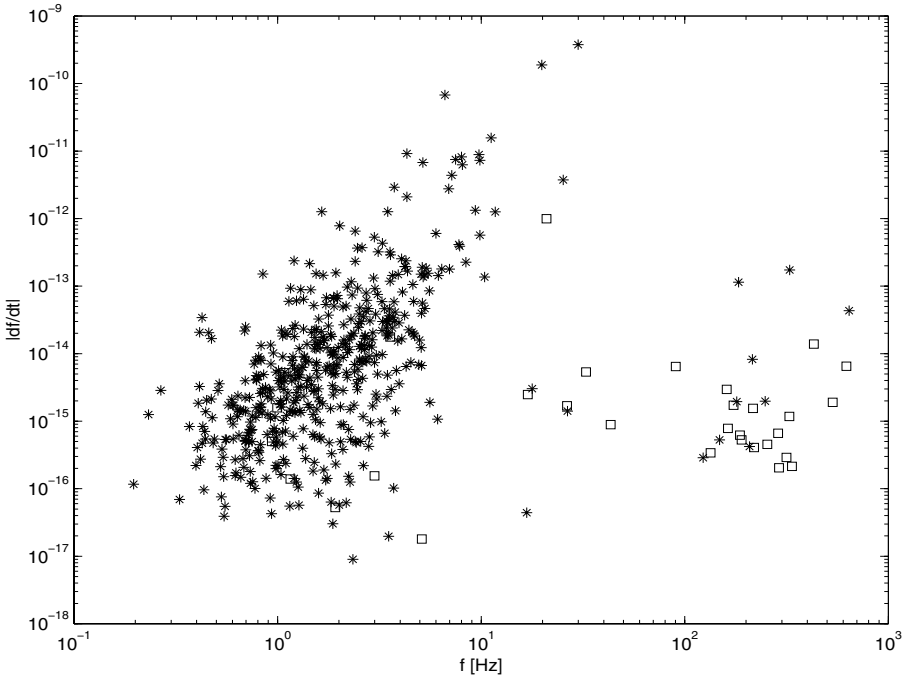

Figure 2: Spin-down rate $\dot{\nu}$ as a function of the frequency ν . The "stars" correspond to normal pulsar, the "squares" to millisecond pulsars.

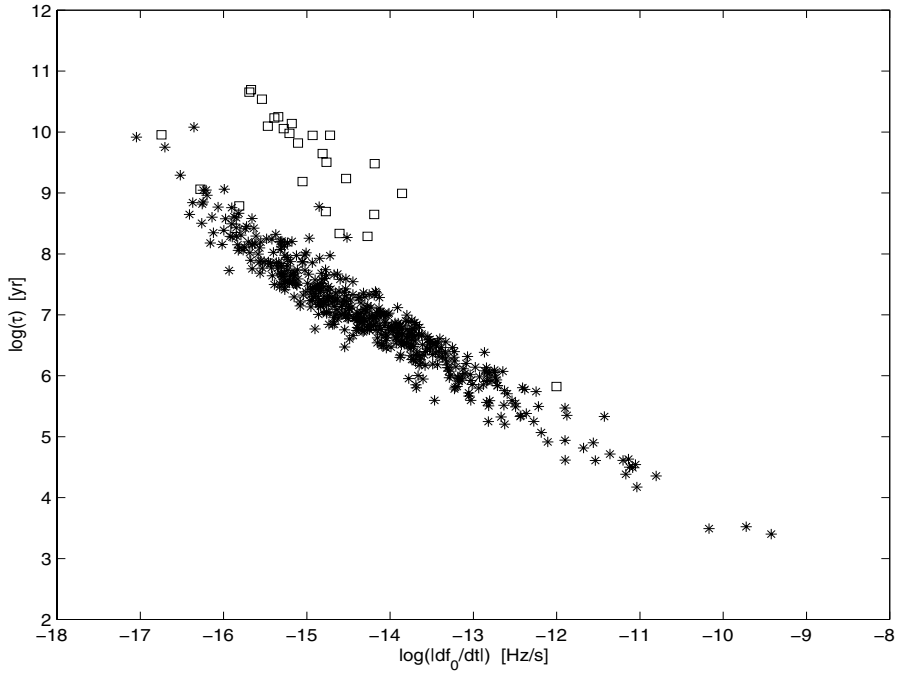

Figure 3: Pulsar spin-down age τ as a function of the spin-down rate $\dot{\nu}$. The "stars" correspond to normal pulsar, the "squares" to millisecond pulsars.

name	$\nu_{rot}\ [Hz]$	h_0	ϵ_{max}	$h_{0,max}$
$Vela$	11	$1.1 \cdot 10^{-27}\epsilon_{-6}$	$1.8 \cdot 10^{-3}$	$1.9 \cdot 10^{-24}$
$Crab$	30	$1.9 \cdot 10^{-27}\epsilon_{-6}$	$7.5 \cdot 10^{-4}$	$1.4 \cdot 10^{-24}$
$Geminga$	4.2	$4.7 \cdot 10^{-28}\epsilon_{-6}$	$2.3 \cdot 10^{-3}$	$1.1 \cdot 10^{-24}$
$PSR\ B1509-68$	6.6	$4.1 \cdot 10^{-29}\epsilon_{-6}$	$1.4 \cdot 10^{-2}$	$5.8 \cdot 10^{-25}$
$PSR\ B1706-44$	10	$2.2 \cdot 10^{-28}\epsilon_{-6}$	$1.9 \cdot 10^{-3}$	$4.2 \cdot 10^{-25}$
$PSR\ B1957+20$	621	$1.1 \cdot 10^{-24}\epsilon_{-6}$	$1.6 \cdot 10^{-9}$	$1.7 \cdot 10^{-27}$
$PSR\ J0437-4715$	174	$9.1 \cdot 10^{-25}\epsilon_{-6}$	$2.9 \cdot 10^{-8}$	$2.6 \cdot 10^{-26}$

Table 1: Gravitational wave data for a sample of pulsars. ν_{rot} is the rotation frequency of the star. The amplitude of the gravitational wave h_0 is expressed in terms of $\epsilon_{-6} = \frac{\epsilon}{10^{-6}}$. The maximum amplitude $h_{0,max}$ is that corresponding to the maximum ellipticity ϵ_{max}. The last two items correspond to millisecond pulsars. Note that, for millisecond pulsars, the upper limits on the ellipticity are much lower than those relative to Crab-like pulsars. From E. Gourgoulhon & S. Bonazzola [5].

significantly from axisymmetry than older one, which, on the contrary, rotate faster and are more likely to have settled into an axisymmetric configuration. As to this respect, from Eq.(16) we see that $h_0 \propto \nu^2 \cdot \epsilon$, so that there is a competition between the frequency of the waves emitted and the ellipticity of the star.

The highest values of h_0, among the ~ 700 galactic pulsars of the catalog by Taylor *et al.*[6] [17], are of the order of $h_0 \sim 10^{-24}$, even if, following what we have said before, the true amplitudes are probably much lower [19].

Among the observed pulsars, more than one hundred have a rotation frequency greater than $4\ Hz$ [15] and then could emit gravitational waves in the sensitivity band of interferometers. For more details on pulsars characteristic parameters, see Sec.(5).

3.3.1 Glitches

Glitches are sudden increases in the angular velocity Ω and in the spin-down rate $\dot{\Omega}$ of a rotating neutron star. Several events have been observed for the Crab, the Vela and some other pulsars. The typical intervals between glitches vary from several months to years. The magnitude of the "jumps" in the rotation and spin-down rate are of the order $\frac{\Delta\Omega}{\Omega} \sim 10^{-8} \div 10^{-6}$ and $\frac{\Delta\dot{\Omega}}{\dot{\Omega}} \sim 10^{-4} \div 10^{-2}$.

[6]However, considering the limits on the sensitivity of radio observations, a total number of galactic active pulsars $\sim 10^5$ is supposed to exist.

Many models have been developed in order to explain the nature and the characteristics of glitches. The persistent increase in the spin-down rate, called *offset*, suggests increases in the spin-down torque acting on the star. This can be a consequence of variations of the direction or the magnitude of the magnetic moment of the star. Such variations could be driven by starquakes occurring when the crust becomes less oblate, as a consequence of spin-down [28], [29]. Repeated starquakes can increase the angle between the rotation and magnetic axes to large values. Another possibility is a reduction of the moment of inertia on which the external torque acts, which could be due to coupling and decoupling processes between different components of the star [30]. According to the *vortex creep theory* [31], for instance, the driving mechanism is the pinning and unpinning of vortices in the superfluid and the lattice of neutron rich nuclei coexisting in the inner crust. Other models involve core-quakes [32] or the sudden annihilation of superfluid vortices at the crust-core interface [33].

3.4 Secular instabilities

Secular nonaxisymmetric instabilities can develop if some dissipative mechanism is at work in a rapidly rotating neutron star. They are called "secular" because the typical timescale over which they develop is much larger than the orbital period.

There are two kinds of secular instabilities: the *Chandrasekhar-Friedman-Schutz instability* (CFS) driven by gravitational radiation reaction [34], [35] and the *viscosity-driven instability* [40], [41].

A pioneering work in this field was that of Chandrasekhar [49], who studied the evolution of rotating incompressible newtonian stars modeled as Maclaurin spheroids[7], which are axisymmetric ellipsoids, and found that a critical parameter is the ratio $\beta = \frac{T}{|W|}$ between the rotational energy and the gravitational potential energy of the star. In particular, the $l = m = 2$ *f-mode*[8] (called "bar" mode) becomes unstable when β is greater than the secular stability limit, $\beta > \beta_{sec} = 0.1375$. This result also holds for polytropic stars[9] [36]. At

[7]The sequence of Maclaurin spheroids describes the equilibrium configurations of a homogeneus body rotating with uniform angular velocity.

[8]f means "fundamental". *f-modes* belong, together with p ("pressure") and g ("gravity") *modes*, to the category of *polar fluid modes*, which are analogous to the Newtonian fluid pulsations.

[9]i.e. stars described by a polytropic equation of state: $P = k\rho^{\gamma}$, with $\gamma = 1 + \frac{1}{n}$; n

this point two branches bifurcate from the axisymmetric Maclaurin sequence: the Jacobi sequence, whose configuration is that of a triaxial ellipsoid rigidly rotating around its smallest axis, and the Dedekind sequence, whose configuration is a fixed triaxial figure with an internal fluid circulation with constant vorticity.

If the CFS instability takes place in an inviscid (i.e. zero viscosity) neutron star, the evolution does not conserve the angular momentum but conserves the fluid circulation around the equator, which we will define below; then, a Mclaurin spheroid evolves toward a Dedekind ellipsoid with the same mass and equatorial circulation. On the other hand, if the instability is driven by viscosity, the angular momentum is conserved but not the circulation. In such a case, the Mclaurin spheroid evolves toward a final state described by a Jacobi ellipsoid, with the same angular momentum and rest mass. The value of β_{sec} is weakly dependent on the politropic index n [36].

For a given star model the value $\beta = \beta_{sec}$ corresponds to a critical rotation frequency $\nu_{sec} = \frac{\Omega_{sec}}{2\pi}$ which must be compared with the Keplerian frequency ν_K corresponding to the mass shed limit: it is the rotation frequency at which the centrifugal force balances the gravitational force at the equator of the star. At frequencies greater than this the star would lose matter from the equator. We have

$$\nu_K \simeq \frac{1}{3\pi}\sqrt{\pi G\overline{\rho}} = 1.25 \cdot 10^3 \left(\frac{M}{1.4M_\odot}\right)^{1/2} \left(\frac{R}{10km}\right)^{-3/2} \quad Hz \tag{51}$$

where M, R are the mass and the radius of the non rotating star. The first equality in Eq.(51), where $\overline{\rho}$ is the mean density of the star, is nearly valid for any equation of state. In Tab.(2) we have reported, from [51], the frequencies ν_{sec} and the ratios $\frac{\nu_{sec}}{\nu_K}$ for different $l = m$ *f-modes* and different politropic index n relative to rigidly rotating newtonian neutron stars. We see that for incompressible spheroids ($n = 0$), the bifurcation point, for the $l = m = 2$ mode, is below the mass shed limit: $\nu_{sec} < \nu_K$. This condition holds also for compressible rigidly rotating spheroids if $n < 0.808$ [61] and mass shed can be inhibited for greater n if a slight amount of differential rotation is allowed [36].

Higher order modes can become unstable at lower values of β_{sec}, but for $\beta \gtrsim 0.17$ their growth time is much larger than that of the "bar" mode (for instance, more than a factor of 10 for the mode $m = 3$) and, above all, the stabilizing effect of viscosity is greater, so that attention is generally focused on

is the *polytropic index*.

$l=m$	n	$\frac{\sigma_m(0)}{\sqrt{\pi G\rho}}$	$\frac{\nu_c}{\sqrt{\pi G\rho}}$	$\frac{\nu_c}{\nu_K}$	β_{sec}
2	0	1.033	0.097	0.913	0.1375
	3/4	1.292	0.102	0.994	0.1298
	1	1.415			
	5/4	1.543			
3	0	1.512	0.088	0.822	0.0991
	3/4	1.819	0.095	0.926	0.0866
	1	1.959	0.097	0.955	0.0800
	5/4	2.095	0.097	0.976	0.0694

Table 2: In this table we have reported, for different $l = m$ *f-modes* and politropic indexes n : the angular frequency of the mode $\sigma_m(0)$ (real part) for a non rotating star; the frequency ν_{sec} corresponding to the bifurcation point $\beta = \beta_{sec}$; the ratio between ν_{sec} and the mass shedding frequency ν_K ; the value of β_{sec} . The neutron star is modeled as a Newtonian, rigidly rotating, inviscid fluid. For the mode $l = m = 2$ and $n = 1, 5/4$, the mass shed limit is reached before the bifurcation point. For more details, see [51]. We have different results for relativistic stars, see text.

the $l = m = 2$ *f-mode*.

General Relativity tends to strengthen the CFS-instability [52]. This means that the critical ratio $\frac{\nu_{sec}}{\nu_K}$ decreases for a given equation of state. An important result is that the maximum polytropic index for which the bar-instability is set below the mass-shed limit is $n \simeq 1.3$ instead of the newtonian value $n = 0.808$ [53]. The value of β_{sec} is also changed in General Relativity. Morsink *et al.* [54] find that, for a wide range of realistic equations of state, β_{sec} can be fitted by the following formula:

$$\beta_{sec} \simeq .115 - 0.048\frac{M}{M_{max}} \tag{52}$$

where M_{max} is the maximum mass for a non rotating star with the same equation of state. For instance, for $1.4\ M_\odot$ neutron stars the $l = m = 2$ *f-mode* becomes unstable at $\beta_{sec} \sim 0.08$, instead of $\beta_{sec} \simeq 0.14$.

There is also a dynamical stability limit for the $l = m = 2$ "bar" mode: this mode becomes dynamically unstable for $\beta \geq \beta_{dyn} = 0.2738$ and the instability, which has been numerically analized, in Newtonian limit, for instance by Houser *et al.* [37], develops on a timescale comparable with the orbital period of the system and it is characterized by a strong emission of gravitational radiation, with efficiency $\epsilon \sim .001$, peaked at high frequency, $\nu \sim 4\ kHz$.

It is possible that a newborn rapidly rotating neutron star first undergoes a

phase of dynamical instability and that the final value of β is still greater than β_{sec}, so that the development of a secular instability follows.

Up to now, calculations of gravitational radiation emitted in the CFS-instability have been performed only for Newtonian polytropic stars [36]. Then, let us define some quantities through which we can describe the different possible evolutionary paths of a given Newtonian ellipsoid. A generic ellipsoid is characterized by the *pattern speed* with respect to a principal axis $\vec{\Omega}_{ps} = \Omega_{ps}\vec{e}_3$, and by the internal motion of the fluid described, in a frame corotating with the ellipsoid, by the *vorticity* $\vec{\zeta} = \zeta\vec{e}_3$. The *pattern speed* gives the angular velocity of star surfaces of constant displacement, as observed by an inertial observer. Indicating by a_1, a_2, a_3 the three principal axes, we define, following Lai & Shapiro [36]

$$\Lambda = -\frac{a_1 \cdot a_2}{(a_1^2 + a_2^2)}\zeta \tag{53}$$

and

$$\mathcal{C} = I\Lambda - \frac{2}{5}k_n M a_1 a_2 \Omega_{ps} \tag{54}$$

where

$$I = \frac{k_n}{5}M(a_1^2 + a_2^2) \tag{55}$$

is the momentum of inertia with respect to the 3-axis and $k_n \leq 1$ is a constant depending on the polytropic index n ; $k_n = 1$ for an incompressible star. $\mathcal{C}$ has the dimensions of an angular momentum and is proportional to the circulation along the equator of the star. Moreover, the angular momentum of the ellipsoid is

$$J = I\Omega_{ps} - \frac{2}{5}k_n M a_1 a_2 \Lambda \tag{56}$$

For a Maclaurin spheroid $a_1 = a_2$, $\zeta = 0$, then $J = I\Omega_{ps} = \mathcal{C}$. For the Jacobi-like sequence $|\zeta| < 2|\Omega_{ps}|$, while for the Dedekind-like sequence $|\zeta| > 2|\Omega_{ps}|$.

The evolution of a given ellipsoid, in the absence of viscosity, takes place along constant-$\mathcal{C}$ sequences and the endpoint depends on the initial value of $\mathcal{C}$. Precisely, let us indicate with $\mathcal{C}_{sec}$ the circulation of a Maclaurin spheroid at the bifurcation point. It has been shown [36] that for a Maclaurin spheroid

$$|\mathcal{C}_{sec}| = J_{sec} = 0.304\sqrt{\frac{k_n M^3 R}{1 - n/5}} \tag{57}$$

If the initial configuration has $\mathcal{C} < \mathcal{C}_{sec}$, i.e. $\beta < \beta_{sec}$, then the axisymmetric Maclaurin spheroid is stable and it is the endpoint of the evolution of both Jacobi and Dedekind ellipsoids. On the other hand, if $\mathcal{C} > \mathcal{C}_{sec}$ the evolution, as we have said before, is toward a Dedekind configuration, for an inviscid neutron star, while the final state is a Jacobi ellipsoid if the viscosity, but not gravitational radiation reaction, is taken into account.

3.4.1 Maclaurin - Dedekind evolution

Let us consider an inviscid neutron star described by a Maclaurin spheroid with $\beta > \beta_{sec}$: in this initial configuration the $l = m = 2$ bar-instability develops, due to gravitational radiation reaction.

In Thorne's words [10] it manifests in the form of "strong hydrodynamic waves in the star's surface layers and mantle, propagating in the opposite direction to the star's rotation".

The frequency of the gravitational waves emitted, twice the pattern frequency, is an increasing function of the angular velocity Ω of the star and is given by

$$\nu(\Omega) = \frac{\Omega - \sigma_2(0)}{2\pi} \tag{58}$$

where $\sigma_2(0)$ is the frequency of the $l = 2$ mode for a non rotating star, see Tab.(2). The *pattern speed* is [36] $\Omega_{ps}(\Omega) = \pi \cdot \nu(\Omega)$. It must be noted that it is always lower than the rotational frequency of the star. The frequency of the waves is maximum at the beginning of the instability and then it decreases monotonically. The gravitatoinal emission is described by Eqs.(12-18).u In Fig.(4), from Lai & Shapiro [36], the gravitational wave amplitude, as a function of the frequency, is plotted for different values of β. The maximum frequency of gravitational radiation depends on the initial value of β and it is as high as $\sim 1\ kHz$ if β is near the dynamical stability limit. At the beginning, the amplitude of the emitted gravitational wave is small, because the star is nearly axisymmetric, then it increases. At the same time the angular velocity Ω decreases and the final configuration is a Dedekind one, a triaxial ellipsoid with zero angular velocity which, clearly, does not emit gravitational radiation. As a result, the amplitude of the wave first increases very rapidly, reaches a maximum, then slowly decreases to zero again. The efficiency is as high as $\sim .02$ if the initial configuration is near the dynamical stability limit. As an example, for a neutron star described by a

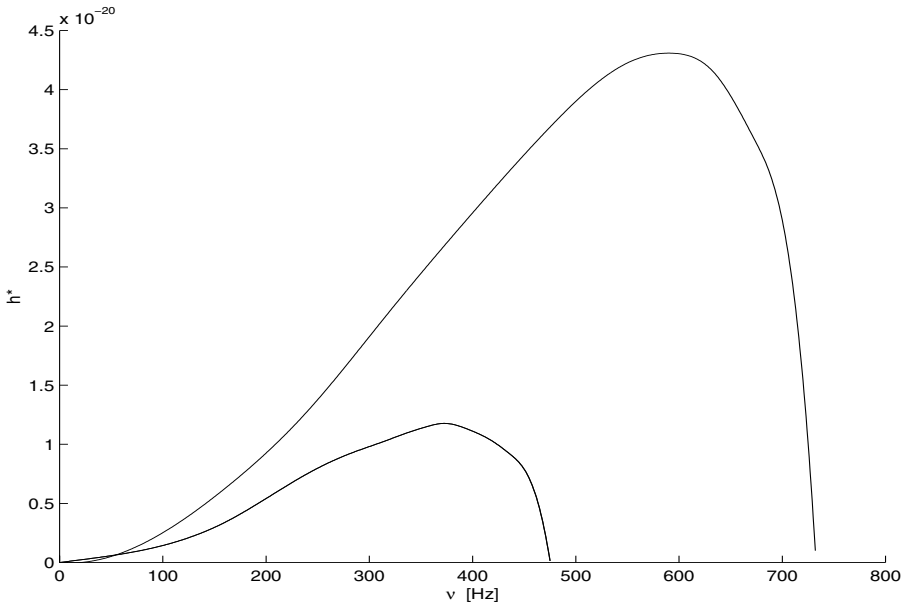

Figure 4: Amplitude of the gravitational wave signal, as a funcion of the frequency, emitted by a secularly unstable neutron star, evolving from a Mclaurin spheroid toward a Dedekind ellipsoid. The upper curve corresponds to $\beta = 0.24$ and the lower one to $\beta = 0.20$, both for a star described by a politropic equation of state with $n = 0.5$. Expliciting the parameters of the source, the amplitude, for a fixed frequency, is $h = h^* \cdot \left(\frac{M}{1.4M_\odot}\right)^2 \left(\frac{10\ km}{R}\right) \left(\frac{10\ kpc}{r}\right)$, where M, R, r are respectively the mass, the radius and the distance of the unperturbed star. From Lai & Shapiro [32].

politropic equation of state with index $n = 1$ and whose initial configuration is a Maclaurin spheroid with $\beta = .24$, the maximum amplitude of the wave signal is

$$h_0 \simeq 4.2 \cdot 10^{-20} \left(\frac{M}{1.4M_\odot}\right)^2 \left(\frac{10\ km}{R}\right) \left(\frac{10\ kpc}{r}\right) \tag{59}$$

reached when the wave frequency is $\nu \simeq 500\ Hz$. The efficiency is $\sim .01$. The number of cycles spent near each frequency is of the order of 10^4 when the amplitude is near the maximum and then rapidly increase ($\sim 10^6$ at $\nu \sim 100\ Hz$). The instability growth time τ_{GW} is weakly dependent on the polytropic index n, while it is sensitively dependent on the initial β : for instance, see fig.1 in [36], for the bar-mode we have a growth timescale $\tau_{GW} \simeq 7 \cdot 10^4\ s$ for $\beta \simeq 0.15$ and $\tau_{GW} \simeq 20\ s$ for $\beta \simeq 0.24$.

3.4.2 Jacobi-Maclaurin evolution

Let us now consider a neutron star, with no viscosity, whose initial configuration is a Jacobi ellipsoid (a triaxial ellipsoid with $|\mathcal{C}| < 2|\Omega|$). Due to gravitational

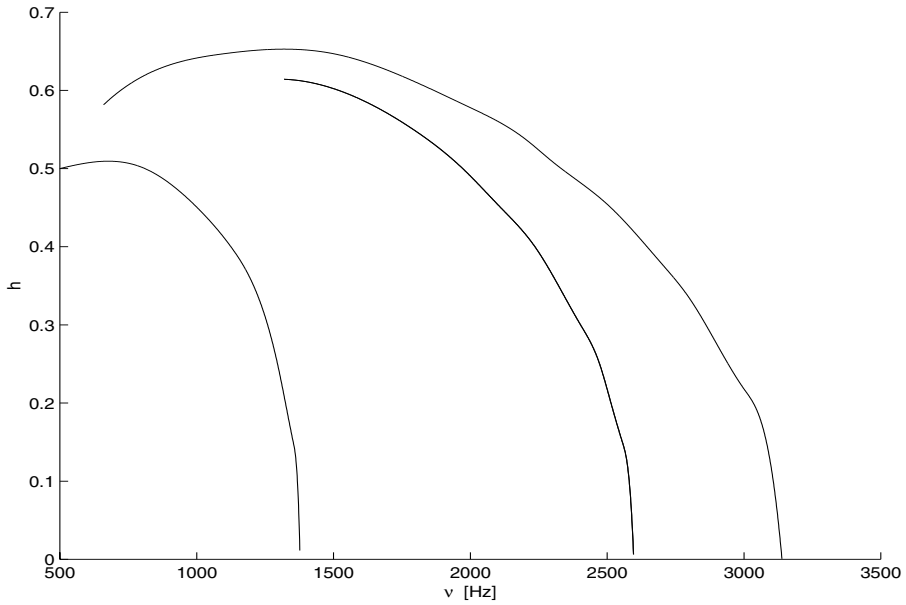

Figure 5: Amplitude of the gravitational wave signal emitted by a secularly unstable neutron star, evolving from a Jacobi ellipsoid toward a Mclaurin spheroid. Moving from up toward down, the three curves correspond to final Mclaurin spheroids with $\beta = 0.02, 0.12, 0.24$ and politropic index $n = 1$. Expliciting the parameters of the source, the amplitude of the wave, for a fixed frequency, is $h = 1.5 \cdot 10^{-18} \cdot h^* \cdot \left(\frac{M}{1.4 M_\odot}\right)^2 \left(\frac{10\ km}{R}\right) \left(\frac{10\ kpc}{r}\right)$, where $M,\ R,\ r$ are respectively the mass, the radius and the distance of the unperturbed star. From Lai & Shapiro [36].

radiation reaction it evolves toward a Maclaurin spheroid and this process is characterized by the emission of a gravitational wave of increasing frequency, the so-called "spio-up" wave. This was first showed by Chandrasekar [38] and is due to the decrease of the momentum of inertia of the star as angular momentum is radiated. For the $l = m = 2$ *f-mode*, the wave frequency is

$$\nu(\Omega) = \frac{\Omega + \sigma_2(0)}{2\pi} \tag{60}$$

where $\sigma_2(0)$ is the Jacobi mode frequency for a non rotating star. The maximum frequency ν_{max} is reached when the ellipsoid approaches the spheroidal shape and it can be as high as $2 \div 3\ kHz$ (depending on the politropic index n) when the final β is low ($\beta \lesssim 0.17$). In Fig.(5), from Lai & Shapiro [36], the amplitude of the gravitational signals emitted during the Jacobi-like evolution is plotted as a function of frequency. For a politropic index $n = 1$ and a final Maclaurin spheroid with $\beta = .12$, for instance, the amplitude has a maximum

value

$$h_0 \simeq 8.7 \cdot 10^{-19} \left(\frac{M}{1.4 M_\odot}\right)^2 \left(\frac{10\ km}{R}\right) \left(\frac{10\ kpc}{r}\right) \tag{61}$$

reached when the frequency of the waves emitted is $\nu \sim 1.3\ kHz$. The wave amplitude is sensibly different from zero up to a frequency $\nu_{max} \sim 2.6\ kHz$. In this case the number of cycles is of order 100 in a large range of frequencies.

If the final Maclaurin spheroid is characterized by $\beta > \beta_{sec}$, a new secular instability, of the kind we have discussed in the preceeding section, will bring from a Maclaurin spheroid to a Dedekind ellipsoid.

The evolution of a Jacobi-like ellipsoid toward a Mclaurin spheroid is generally much faster than the evolution from un unstable Mclaurin spheroid toward a stable Dedekind ellipsoid. Moreover, the amplitude of the gravitational waves emitted is typically more than 10 times greater.

It is not still clear if the "Jacobi-like waveform" is likely to be emitted during the evolution of a newborn neutron star. It depends on the asymmetry of the neutron star shape following the collapse or the dynamical instability phase. 3-D simulations are needed.

3.4.3 The effects of viscosity

Viscosity drives a different kind of nonaxisymmetric instability in rotating stars, which, as we have said in Sec.(3.4), does not conserve the fluid circulation. General relativistic effects, which strengthen the CFS-instability, however, suppress the viscosity driven instability, so that it can take place only for cold neutron stars described by very stiff equation of state [39].

It is not still completely clear which is the importance of viscosity in neutron stars. In the first tens of seconds after the star's birth, when the instability processes we have discussed are thought to be at work, the temperature of the neutron star is very high, $T \gtrsim 10^{10}\ K$. The bulk viscosity could have some effects in suppressing the CFS instability at temperature greater than $\sim 2 \cdot 10^{10}\ K$ [50], but this result holds for uniformly rotating models and is based on some approximations which should be analyzed more deeply [36].

On the other hand, when the temperature is below $\sim 10^6 \div 10^7\ K$ the shear viscosity should suppresses the CFS instability [12], [52]. Moreover, "mutual friction" in the superfluid interior of neutron stars could suppress the CFS instability at temperature below $\sim 10^8 \div 10^9\ K$, depending on the theoretical model

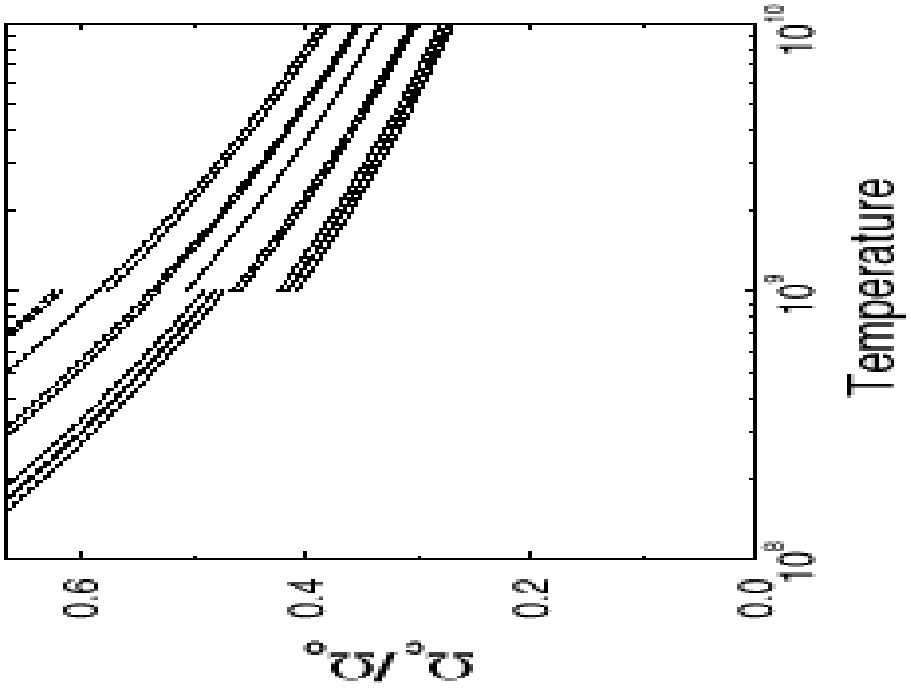

Figure 6: Critical angular velocity Ω_c for different realistic equations of state and for a neutron star of $1.4\ M_\odot$ as a function of temperature. The discontinuity at $T \sim 10^9\ K$ corresponds to the superfluid transition. $\Omega_0 = \sqrt{\pi G \overline{\rho}}$. From L. Lindblom *et al.* [57].

adopted for superfluidity [56], [52]. Then, the CFS instability should be mainly at work in hot newborn neutron stars, while the viscosity-driven instability could be more effective in cold neutron stars and could take place, for instance, during the accretion of matter from a companion star.

3.4.4 r-modes instability

The *r-modes*, which are axial fluid oscillations, governed by the Coriolis force and whose coupling takes place through the current multipoles, instead of the mass multipoles [42], [43], [44], [45], [46], are intensively studied from few years. As for *f-modes*, gravitational radiation makes a *r-modes* unstable if the gravitational radiation time scale is smaller, in absolute value, with respect to the viscous time scale. This condition is verified if the angular velocity of the star is greater than a critical value Ω_c depending on the star temperature, see Fig.(6). This critical frequency for *r-modes* excitation can be strongly modified by the presence of a solid crust. In this case [57] the viscous boundary layer under the crust dramatically increases the viscous damping rate of fluid *r-modes*. On the other hand, Lindblom *et al.* [58] have shown that energy generation in the boundary

layer heats the star and can melt the solid crust if the modes amplitude is high enough ($\alpha > 5 \cdot 10^{-3}$). If this happens, the outer layers can be mainteined in a mixed solid-fluid state until the crust solidifies. In this case, the frequency range spanned by the unstable star should be very similar to that found for a completely fluid star. Also the presence of a magnetic field can have large influence on the development of r-mode instabilities. According to Rezzolla *et al.* [59] for fields $B > 10^{16} \left(\frac{\Omega}{\Omega_k}\right) G$, where $\Omega_k \sim \sqrt{\pi G \overline{\rho}}$ is the mass-shed limit on angular velocity, the *r-modes* are completely suppressed while for much lower fields they are damped on much shorter timescales than found without magnetic field. As a conclusion, now it is not so clear that *r-modes* instabilities are indeed so strong sources of gravitational radiation, as it appeared when they were found. However, more work is needed to have a definite answer. In the following, we give the main relations describing the gravitational wave emission from *r-mode* instability in a fluid politropic star.

The *r-modes*, which exist only if $l = m$, can be described as "large scale oscillating currents that approximatively moves along the equipotential surfaces of the rotating star" [46]; this is why they are also called *convective modes*.

At the lowest order in the angular velocity of the star Ω the frequency of a mode of harmonic index $l = m$ is

$$\sigma_m(\Omega) = -\frac{(m-1)(m+2)}{(m+1)}\Omega \tag{62}$$

and the frequency of the gravitational waves emitted is

$$\nu(\Omega) = -\frac{\sigma_m(\Omega)}{2\pi} \tag{63}$$

The amplitude of the mode is small at the beginning but then it increases, as hydrodinamic effects become important, and a non-linear evolution regime is reached.

During the initial phase of linear evolution the angular velocity of the star, and then the frequency ν of the gravitational signal emitted, is nearly constant:

$$\dot{\nu} \approx -2.7\frac{\alpha^2}{t}\left(\frac{\nu}{1\ kHz}\right)^3 \quad \frac{Hz}{s} \tag{64}$$

and the amplitude α of the mode grows exponentially. As a consequence, the amplitude of the gravitational wave reaches a maximum given by

$$h_0 \approx 4.4 \cdot 10^{-24}\left(\frac{\Omega_0}{\sqrt{\pi G \overline{\rho}}}\right)^3 \left(\frac{20\ Mpc}{r}\right) \tag{65}$$

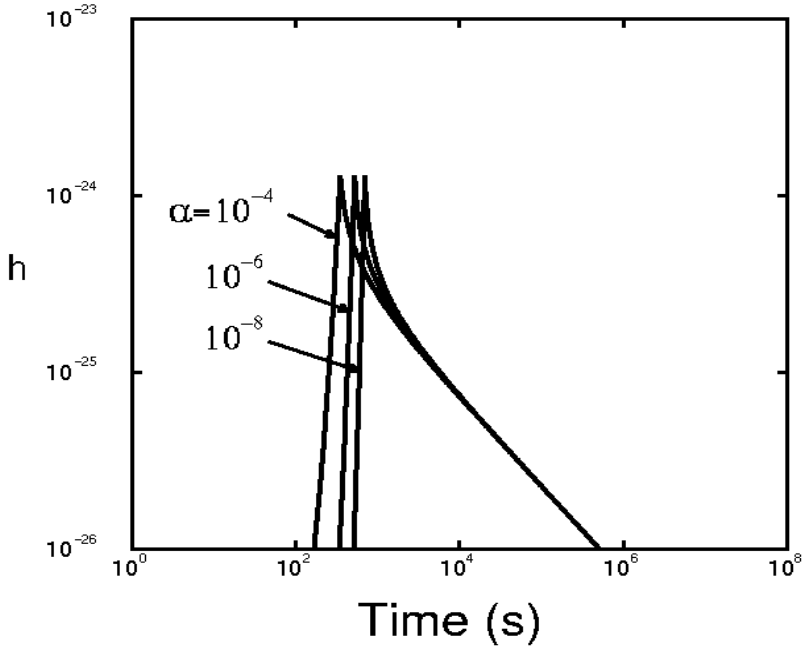

Figure 7: The gravitational wave signal emitted when the *r-mode* instability is excited in a fluid star, for different values of the initial size of the perturbation α. The distance is $r = 20\ Mpc$ and the initial angular velocity of the star is equal to the mass-shedding limit: $\Omega_0 = \Omega_K$. From B. J. Owen *et al.* [22].

where $\sqrt{\pi G\overline{\rho}} \simeq 8 \cdot 10^3 \left(\frac{\overline{\rho}}{3 \cdot 10^{14} g/cm^3}\right)^{1/2}\ rad \cdot s^{-1}$ and Ω_0 is the initial angular velocity of the star; the corresponding gravitational frequency for the mode $l = m = 2$ is $\nu = \frac{2\Omega_0}{3\pi}$.

When the non-linear phase is reached, probably a saturation effects occurs and the mode no longer growths. At that point the excess angular momentum of the star is radiated away through gravitational radiation and the star spins down until angular velocity and temperature are sufficiently small so that the crust solidifies and r-modes are completely damped. The amplitude of the gravitational signal emitted decreases according to

$$h(t) = 4.4 \cdot 10^{-24} \left(\frac{\Omega(t)}{\sqrt{\pi G\overline{\rho}}}\right)^3 \left(\frac{20\ Mpc}{r}\right) \tag{66}$$

In this non linear phase the time variation law for the wave frequency is

$$\dot{\nu} \approx -1.8 \left(\frac{\nu}{1\ kHz}\right)^7 \quad \frac{Hz}{s} \tag{67}$$

4 Accreting neutron stars

4.1 CFS secular instability

Let us consider a binary system composed of a neutron star and an ordinary star filling its Roche lobe: an accretion disk forms around the compact object which accretes both matter and angular momentum. The increase of angular momentum must be compared with the decrease connected with the pulsar mechanism or other dissipative effects. If the magnetic field is significantly lower than the canonical value $\sim 10^{12}\ G$, the accretion process can be dominant and the angular velocity of the neutron star (or, equivalently, $\beta = \frac{T}{|W|}$) can reach the critical value at which the CFS secular instability develops determining a strong emission of gravitational waves. The triaxial deformation of the neutron star changes in such a way that the loss of angular momentum through gravitational radiation exactly balances the accretion of angular momentum (due to accretion of matter): a quasi-steady state is reached, in which the angular velocity of the star no longer grows. This mechanism was first proposed by Wagoner [47].

The loss of angular momentum through gravitational waves is

$$\left(\frac{dJ}{dt}\right)_{GR} = \left(\frac{1}{\Omega_{ps}}\frac{dE}{dt}\right)_{GR} = \pi G c^3 r^2 h^2 m \nu \tag{68}$$

where h is the amplitude of the wave emitted and $\nu = \frac{m\Omega_{ps}}{2\pi}$ is the frequency of gravitational waves, see Eq.(58), depending, as we know, on the mode which is destabilized (with the underlying hypotesis $l = m$) and on the pattern speed Ω_{ps}.

Equating Eq.(68) to the accretion rate of the angular momentum we can write [47]

$$h \simeq 2{\cdot}10^{-27} \left(\frac{M}{1.4\ M_\odot}\right)^{1/4} \left(\frac{R}{10\ km}\right)^{1/4} \left(\frac{1\ kHz}{m\nu}\right)^{1/2} \left(\frac{10\ kpc}{r}\right) \left(\frac{\dot{M}}{10^{-8}\ M_\odot/yr}\right)^{1/2} \tag{69}$$

where $\dot{M}$ is the matter accretion rate. For the $l = m = 2$ *f-mode* we expect $\nu \lesssim 800\ Hz$, see Sec.(3.4).

We can express $\dot{M}$ in terms of the X-ray luminosity through the approximate relation [47]

$$F_X = \frac{1}{4\pi r^2}\left(\frac{dE}{dt}\right)_\gamma \approx \frac{3GM}{16\pi R r^2}\dot{M} \tag{70}$$

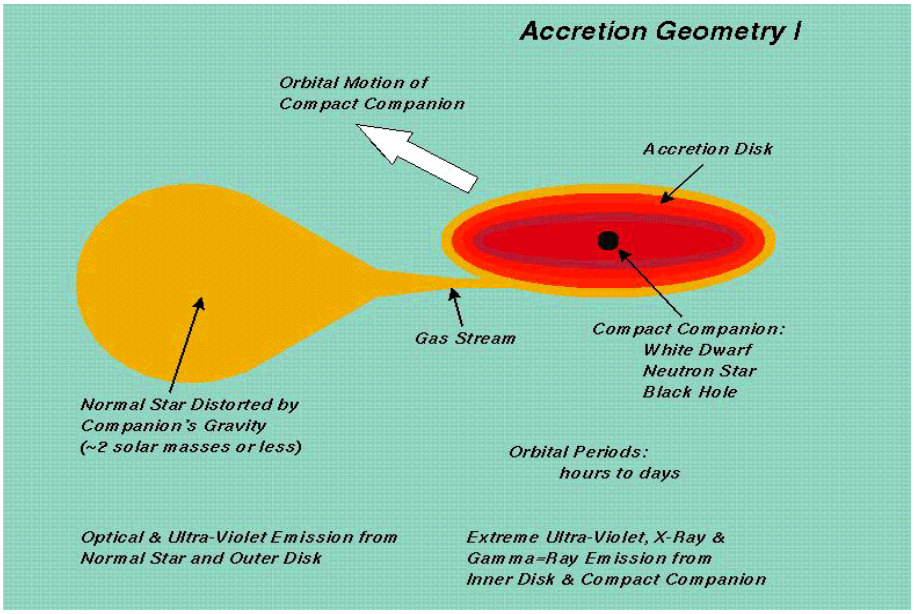

Figure 8: X-ray binary system: matter flows through the Roche lobe from the normal star and is accreted by the compact star. Picture taken at the *Marshall Space Flight Center* web site http://xanth.msfc.nasa.gov/xray/openhouse/ns/.

obtaining

$$h \approx 2.8 \cdot 10^{-27} \left(\frac{M}{1.4\ M_\odot}\right)^{-1/4} \left(\frac{R}{10\ km}\right)^{3/4} \left(\frac{1\ kHz}{m\nu}\right)^{1/2} \left(\frac{F_X}{10^{-8}\ erg\ cm^{-2}\ s^{-1}}\right)^{1/2} \tag{71}$$

See the section on data bases and ref.[66] for a discussion on the importance of following the variations of the accretion rate $\dot{M}$ and on its connection with the s_Z parameter in the X-ray color-color diagrams of low mass X-ray binaries.

Let us now compare these results with observations. The data of the *Rossi X-Ray Timing Explorer* (RXTE) strongly suggest that several rapidly accreting and weakly magnetic neutron stars ($\dot{M} > 10^{-11}\ M_\odot\ yr^{-1}$, $B \ll 10^{11}\ G$) are rapidly rotating with frequency $\nu_{rot} > 250\ Hz$. More precisely, they all rotate with frequency between 250 and $600\ Hz$, with most in a narrow band around $300\ Hz$ [65]. For such systems the CFS-instability connected with *f-modes* cannot be at work, even if viscosity is absent. Let us see alternative explanations.

4.2 r-modes instability

A spinning up accreting neutron star could reach angular velocities at which *r-modes* are unstable and then emit gravitational radiation in a quasi stationary regime in which all accreted angular momentum is radiated away. This mechanism of emission has been analyzed by N. Andersson *et al.* [62].

For a normal fluid, uniform density star, the critical period below which the instability can set in is given by [62]

$$P_c \approx 2.8 \left(\frac{R}{10km}\right)^{39/24} \left(\frac{M}{1.4M_\odot}\right)^{-1/24} \left(\frac{T}{10^7 K}\right)^{1/3}\ ms \tag{72}$$

corresponding to a rotational frequency

$$\nu_c \approx 360 \left(\frac{R}{10km}\right)^{-39/24} \left(\frac{M}{1.4M_\odot}\right)^{1/24} \left(\frac{T}{10^7 K}\right)^{-1/3}\ Hz \tag{73}$$

Then, as we have previously underlined, neutron stars become unstable, if the crust is not solidified and neglecting the effects of a magnetic field, at angular velocities lower than those typical of *f-modes* instabilities. These results have been compared in [62] with data relative to (recycled) millisecond pulsars and low mass X-ray binary systems. According to the standard scenario millisecond pulsars are the final product of low mass X-ray binary systems (LMXB) in which the

neutron stars spun up to high angular velocity accreting matter from a low mass companion. This model is now receiving support from the recent observations of chilohertz quasi periodic oscillations (QPO) [63] which suggest that neutron stars in LMXB are rapidly spinning and from the discovery of the X-ray pulsar $SAX\ J1808.4-3658$ with a period $P \simeq 2.49\ ms$ [64]. Particularly important is the fact that many neutron stars in LMXB are rotating with similar angular velocity, with most in the range $260 \div 330\ Hz$. It is possible that such neutron stars' rotation rate is limited by the *r-mode* instability, see Eq.(73), and the observed periods and upper limits on the surface temperature of millisecond pulsars do not contradict this conclusion. N. Andersson *et al.* [62] find for the amplitude of the gravitational signal emitted

$$h_0 \approx 4.2 \cdot 10^{-27} \left(\frac{R}{10km}\right)^{1/4} \left(\frac{M}{1.4M_\odot}\right)^{1/4} \left(\frac{300Hz}{\nu_{rot}}\right)^{1/2} \left(\frac{r}{10kpc}\right)^{-1} \tag{74}$$

4.3 Asymmetric temperature distribution

Bildsten [65] has proposed a different mechanism in order to explain the apparent clustering of accreting neutron star rotation frequencies around $\sim 300\ Hz$. He suggests that accreting neutron stars have a misaligned quadrupole moment, with respect to the rotation axis, so that the resulting gravitational wave emission prevents the star from being spun up any further: again, an equilibrium is reached between the angular momentum accreted and that radiated away. The strong dependence of the power emitted in gravitational waves from the rotation velocity of the star ($\dot{E} \propto \Omega^6$, see Eq.(42)) can explain in a natural way why the spin frequencies are similar.

Regarding the origin of the misaligned quadrupole moment, if the star possesses an asymmetric temperature distribution, connected for instance, but not necessarily, with the accretion process, then the electron capture from the nuclei in the crust, which is temperature sensitive, induces a density asymmetry and then a misaligned quadrupole moment.

Starting from eq.(1) of Bildsten [65], we can approximately express the amplitude of gravitational wave signals as

$$h_0 \approx 2.4 \cdot 10^{-27} \left(\frac{M}{1.4\ M_\odot}\right)^{-1/4} \left(\frac{R}{10\ km}\right)^{3/4} \left(\frac{\dot{M}}{10^{-9}\ M_\odot/yr}\right)^{1/2} \left(\frac{300Hz}{\nu}\right)^{1/2} \left(\frac{10kpc}{r}\right) \tag{75}$$

Now, assuming a neutron star luminosity $L = F_X \cdot 4\pi r^2 \approx \frac{3GM\dot{M}}{4R}$ we can write

$$h_0 \approx 9 \cdot 10^{-27} \left(\frac{M}{1.4\ M_\odot}\right)^{-1/4} \left(\frac{R}{10\ km}\right)^{3/4} \left(\frac{300Hz}{\nu}\right)^{1/2} \left(\frac{F_X}{10^{-8}\ erg\ cm^{-2}\ s^{-1}}\right)^{1/2} \tag{76}$$

The strongest known X-ray source is $Sco\ X-1$ whose X-ray flux is $F_X \simeq 2 \cdot 10^{-7}\ erg\ cm^{-2}\ s^{-1}$ [47],[48] but whose spin frequency is still uncertain. Assuming a rotation frequency of $\sim 250\ Hz$ we would have an ampliude $h_0 \sim 3 \cdot 10^{-26}$ with a wave frequency $\nu \sim 500\ Hz$.

5 Parameters of galactic pulsars

In preceeding sections we have described various mechanisms of emission of gravitational radiation which could be at work mainly in neutron stars. In this section we describe with more details the characteristic parameters of galactic pulsars.

Up to date, the most complete catalog is that of Taylor *et al.* [17] containing 706 pulsars (5 of which are extragalactic). Anyway, as we have said in Sec.(3.3), $\sim 10^5$ active pulsars are expected in the Galaxy. The measured rotational frequencies of pulsars are approximately in the range $1 \div 1000\ Hz$, with more than 50 having a period less than $25\ ms$. The fastest pulsar, and also the first millisecond pulsar observed, is $PSR\,B1937{+}21$ whose period is $P = 1.5578\,ms$. In Fig.(9) we have plotted the cumulative distribution function for observed pulsar frequency: we have that $\sim 14\%$ of pulsars have frequency greater than $10\ Hz$, while this fraction rises to $\sim 45\%$ if we consider a lower cut-off equal to $4\ Hz$.

The frequency of gravitational waves emitted by a rotating neutron star is strictly linked to its rotation frequency (for instance, it is $2\nu_{rot}$ for a nonaxisymmetric neutron star rotating around a principal axis, see Sec.(3.1)). Then, any indetermination $\Delta\nu_{rot}$ in the rotation frequency of the star corresponds to an indetermination in the gravitational wave frequency. In connection with the targeted detection strategy of gravitational signal, $\Delta\nu_{rot}$ must be compared with the frequency resolution, which depends on the integration time of the detector:

$$\Delta\nu_{res} \simeq 3 \cdot 10^{-8} \left(\frac{T_{int}}{1\ yr}\right)^{-1} \tag{77}$$

In Fig.(10) the indeterminations on the rotation frequency of observed pulsars have been plotted as a function of their frequency. We see that the values of $\Delta\nu_{rot}$

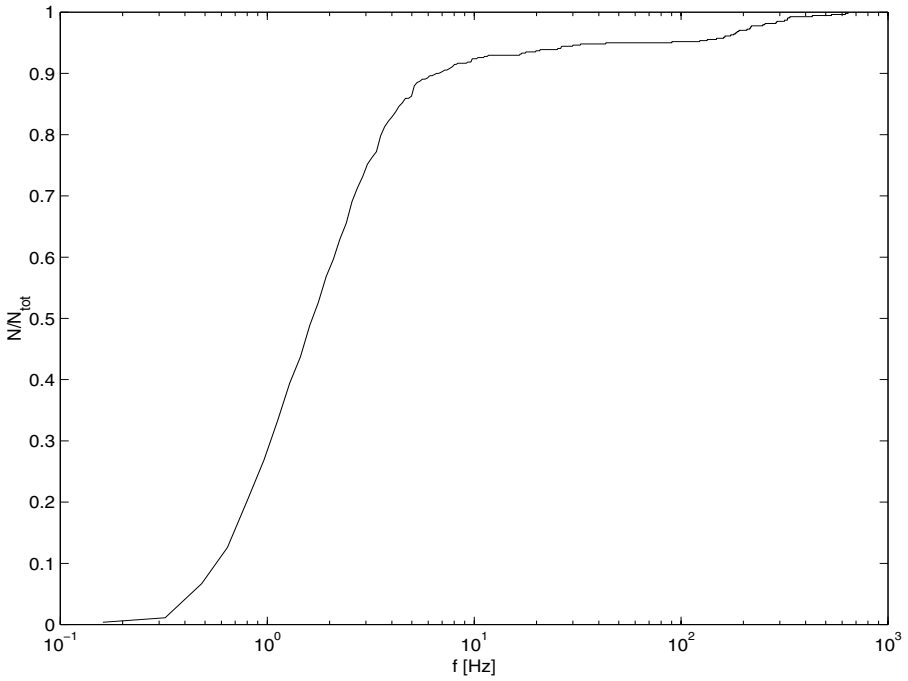

Figure 9: Cumulative distribution for rotation frequency of observed pulsars.

are mainly concentrated into two "bumps". In the biggest one, containing $\sim 60\%$ of the whole survey population, $\Delta\nu_{rot} < \Delta\nu_{res}$ so that this indetermination can be neglected. The other group, characterized by $\Delta\nu_{rot} > \Delta\nu_{res}$, comprises more recently discovered pulsars, which have been monitored for a shorter time. Another important aspect is that of the space distribution of pulsars. In Fig.(11), from [69], the position of observed pulsars in Galactic coordinates α, δ , has been plotted. They are mainly distribuited along the galactic plane. More precisely, $\sim 45\%$ of the single pulsars are concentrated in the region $-\frac{\pi}{2} < \alpha < \frac{\pi}{2}$ and $-.1\ rad < \delta < .1\ rad$ [70].

The precision with which the position of a pulsar is known is critical when the Doppler modulation of the gravitational signal emitted must be taken into account, see the section on the Doppler effect. In Fig.(12) the indeterminations on the position of observed pulsars, in steradians, is reported as a function of the rotation frequency. Again, two "high density" regions come out.

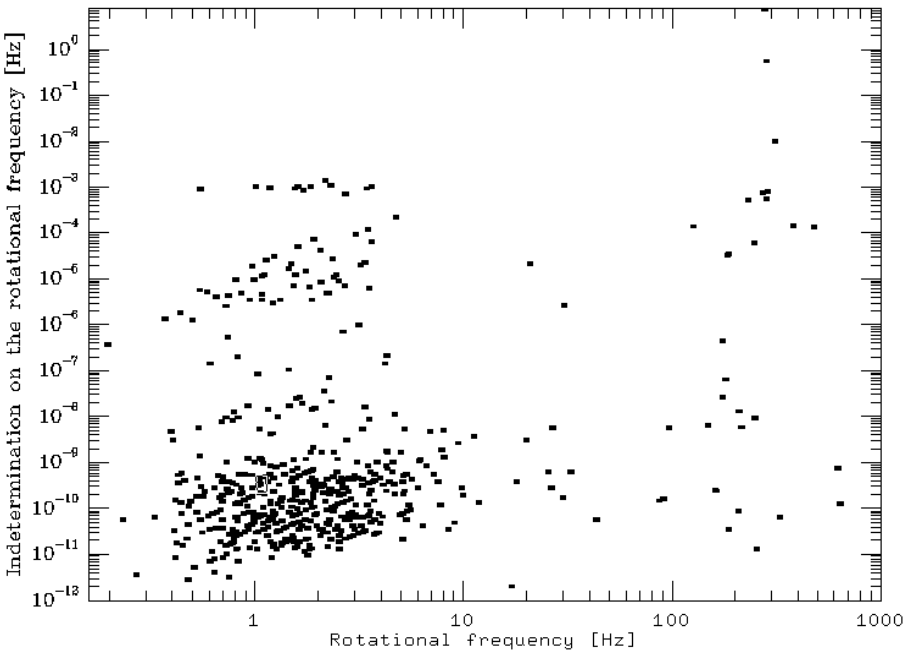

Figure 10: Indetermination in the rotation frequency of pulsars.

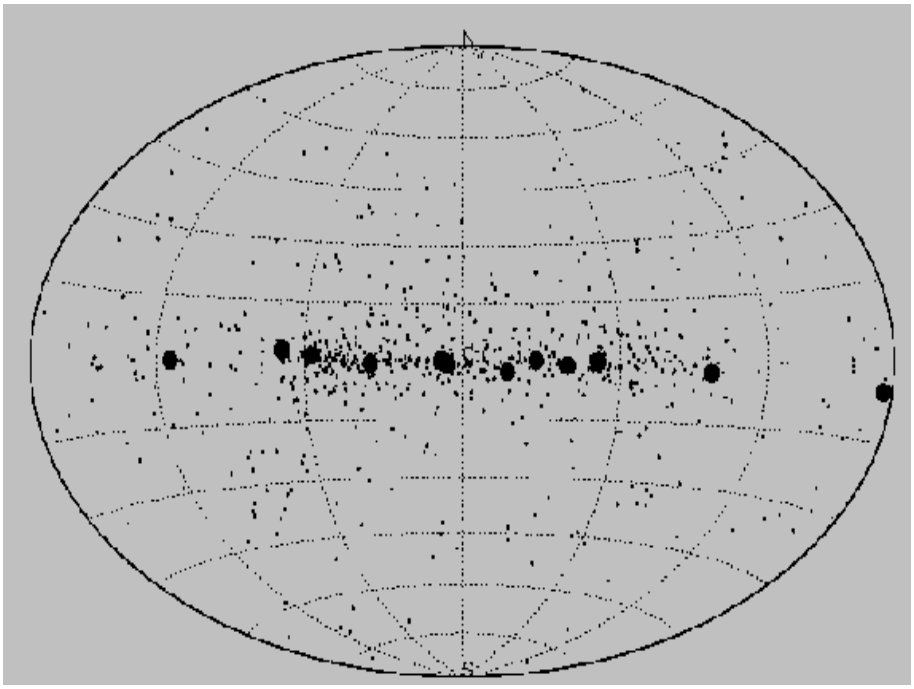

Figure 11: The sky distribution of pulsars in Galactic coordinates. The bold points corresponds to pulsars connected with supernova remnants. From ref.[37].

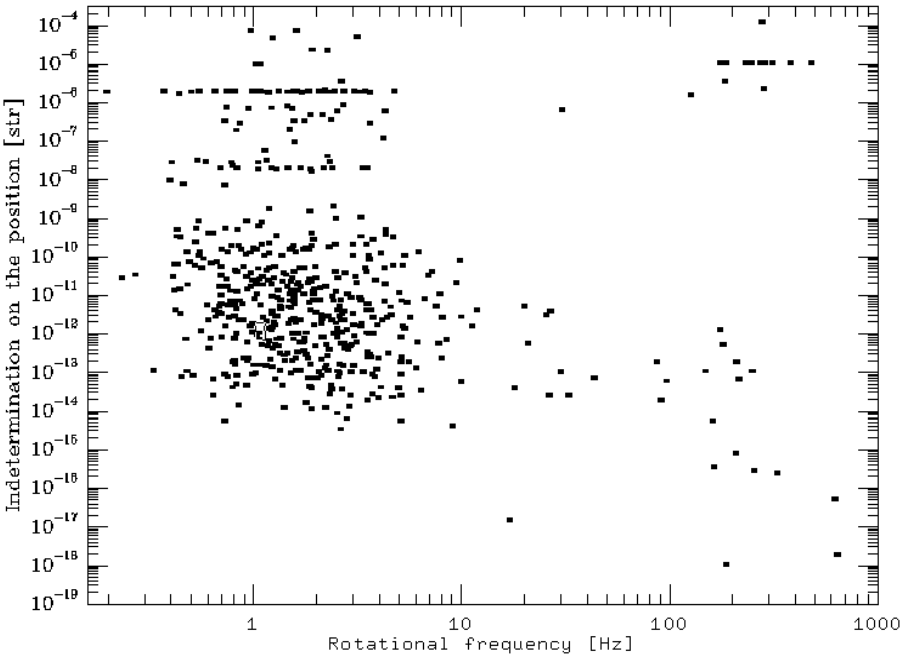

Figure 12: Indeterminations of pulsars position as a function of their rotational frequency

6 References

References

[1] J. van Paradijs, *The lives of the neutron stars*, M. A. Ulpar, U. Kiziloglu, J. van Paradijs (eds), Kluwer Academic Publisher, Dordrecht (1995).

[2] F. M. Walter *et al.*, *Nature*, **379**, 233, 1996.

[3] J. O. Goussard *et al.*, *Astron. & Astrophys.*, **330**, 1005, 1998.

[4] G. Mendell, *Mon. Not. R. Astron. Soc*, **296**, 903, 1998.

[5] V. R. Pandharipande *et al.*, *Nucl. Phys.*, **A 237**, 507, 1976.

[6] T. Takatsuka *et al.*, *Prog. Theor. Phys.*, **60**, 1753, 1978.

[7] M. Kutschera & W. Wojcik, *Nucl. Phys.*, **A 581**, 706, 1995.

[8] G. E. Brown & H. A. Bethe, *The Astrophysical Journal*, **423**, 659, 1994.

[9] F. X. Timmes *et al.*, *The Astrophysical Journal*, **457**, 834, 1996.

[10] K. Torne, *Three Hundreds Years of Gravitation*, Cambridge University Press, 1987.

[11] K. Thorne, *Rev. of Mod. Phys.*, **52**, 299, 1980.

[12] S. Bonazzola & E. Gourgoulhon, *Astron. & Astrophys.*, **312**, 675, 1996.

[13] P. Haensel, Lecture delivered at *Les Houches Summer School*, eds. J.-A.Marck and J.-P.Lasota, 1995.

[14] E. Gourgoulhon & S. Bonazzola, Proceedings of *Gravitational Waves: Sources and Detectors*, eds. E. Ciufolini & F. Fidecaro, World Scientific, 1996.

[15] F. Ricci & A. Brillet, *Annu. Rev. Part. Sci.*, **47**, 111, 1997.

[16] P. R. Brady *et al.*, *Phys. Rev. D*, **57**, 2101, 1998.

[17] J. H. Taylor *et al.*, *The Astrophysical Journal Suppl.*, **88**, 529, 1993.

[18] K. Konno, T. Obata & Y. Kojima, *Astronomy & Astrophysics*, **356**, 234, 2000

[19] A. Giazzotto *et al.*, *Phys. Rev. D*, **55**, 2014, 1997.

[20] K. New, G. Chanmugam, W. W. Johnson & J. E. Tohline, *The Astrophysical Journal*, **450**, 757, 1995.

[21] M .Zimmermann & E. Szedenits, *Phys. Rev. D*, **20**, 351, 1979.

[22] C. Cutler & D. I. Jones, submitted to *Phys. Rev. D*, preprint astro-ph/0008021

[23] J. C. N. de Araujo *et al.*, *Mon. Not. R. Astron. Soc.*, **271**, L31, 1994.

[24] W. Velloso *et al.*, Proceedings of the *XII Italian Conference on General Relativity and Gravitational Physics*, World Scientific, 1996,

[25] A. G. Lyne, R. S. Pritchard, F. G. Smith, *Mon. Not. R. Astron. Soc.*, **233**, 667, 1988.

[26] A. Muslimov & D. Page, *The Astrophysical Journal*, **458**, 347, 1996.

[27] M. P. Allen & J. E. Horvath, *Mon. Not. R. Astron. Soc.*, **287**, 615, 1997.

[28] M. Ruderman, *Nature*, **223**, 597, 1969.

[29] B. Link *et al.*, submitted to *The Astrophysical Journal Letters*, 1998.

[30] S. Balberg *et al.*, to be published in *The Astrophysical Journal Suppl.*, 1998.

[31] M. A. Alpar & D. Pines, in *Isolated Pulsars*, eds. K. A. Van Riper, R. I. Epstein & c. Ho, (Cambridge University Press), 1993.

[32] M. Ruderman, *The Astrophysical Journal*, **382**, 576, 1991.

[33] A. Sedrakian & J. Cordes, in the Proceedings of the 18^{th} Texas Symposium on Relativistic Astrophysics; eds. A. Olinto, J. Frieman & D. Schramm, World Scientific Press, 1997.

[34] S. Chandrasekhar, *Phys. Rev. Lett.*, **24**, 611, 1970.

[35] J. L. Friedman & B. F. Schutz, *The Astrophysical Journal*, **222**, 281, 1978.

[36] D. Lai & S. L. Shapiro, *The Astrophysical Journal*, **442**, 259, 1995.

[37] J. L. Houser *et al.*, *Phys. Rev. Lett.*, **72**, 1314, 1994.

[38] S. Chandrasekhar, *The Astrophysical Journal*, **161**, 571, 1970.

[39] S. Bonazzola, J. Frieben & E. Gourgoulhon, *Atron. Astrophys.*, **331**, 280, 1998.

[40] P. H. Roberts & K. Stewartson, *The Astrophysical Journal*, **137**, 777, 1963.

[41] S. Bonazzola *et al.*, *The Astrophysical Journal*, **460**, 379, 1996.

[42] N. Andersson, gr-qc/9706075, to appear in *The Astrophysical Journal*, 1998.

[43] J. L. Friedman & S. M. Morsink, gr-qc/9706073, to appear in *The Astrophysical Journal*, 1998.

[44] L. Lindblom *et al.*, *Phys. Rev. Lett.*, **80**, 4843, 1998.

[45] N. Andersson *et al.*, in preparation, 1998.

[46] B. J. Owen *et al.*, gr-qc/9804044, to appear in *Phys. Rev. D58*, 084020, 1998.

[47] R. V. Wagoner, *The Astrophysical Journal*, **278**, 345, 1984.

[48] S. Bonazzola & J. A. Marck, *Annu, Rev. Nucl. Part. Sci.*, **45**, 655, 1994.

[49] S. Chandrasekhar, Ellipsoidal Figures of Equilibrium, Yale Univ. Press, 1969.

[50] J. R. Ipser & L. Lindblom, *The Astrophysical Journal*, **373**, 213, 1991.

[51] J. R. Ipser & L. Lindblom, *The Astrophysical Journal*, **355**, 226, 1990.

[52] N. Stergioulas, *Living Reviews in Relativity*, **1**, 8, 1, 1998.

[53] N. Stergioulas & J. L. Friedman, *The Astrophysical Journal*, **492**, 301, 1998.

[54] S. Morsink, N. Stergioulas & S. Blattning, gr-qc/9806008.

[55] K. S. Thorne, *Proceedings of IAU Symposium 165, Compact Stars in Binaries*, edited by J. van Paradijs, E. van den Heuvel, and E. Kuulkers (Kluwer Academic Publishers), 1995.

[56] L .Lindblom & G. Mendell, *The Astrophysical Journal*, **444**, 804, 1995.

[57] L. Bildstein & G. Ushomirsky, *The Astrophysical Journal*, **529**, L33, 2000

[58] L. Lindblom, B. J. Owen & G. Ushomirsky, submitted to *Phys. Rev. D*, 2000

[59] L. Rezzolla, F. Lamb & S. L. Shapiro, *The Astrophysical Journal*, **531**, L141, 2000

[60] S. L. Shapiro & S. A. Teukolsky, *Black Holes, White Dwarfs and Neutron Stars*, (New York: Wiley), 1983.

[61] R. A. James, *The Astrophysical Journal*, **140**, 552, 1964.

[62] N. Andersson *et al.*, astro-ph/9806089, to appear in *The Astrophysical Journal*, 1998.

[63] M. van der Klis, in *Themany faces of neutron stars*, 1997.

[64] R. Wijnands & M. van der Klis, astro-ph/9804216, submited to *Nature*, 1998.

[65] L. Bildsten, to appear in *The Astrophysical Journal Letters*, 1998.

[66] P. Hertz *et al.*, *The Astrophysical Journal*, **396**, 201, 1992.

[67] S. F. Portegies Zwart & L. R. Yungelson, *Astronm. & Astrophys.*, **332**, 173, 1998.

[68] M. Beccaria *et al.*, *Virgo Note NTS96 024*, 1996.

[69] D. R. Lorimer, *Living Reviews in Relativity*, **1**, n.10, 1998.

[70] X. Grave, Ph.D Thesis, 1997.